IL NUOVO CIMENTO **42 C** (2019) 60
DOI 10.1393/ncc/i2019-19060-7

Colloquia: EuNPC 2018

The cryogenic stopping cell of the IGISOL facility at ELI-NP

P. Constantin([1]), A. Rotaru([2]), A. State([2]), D. Nichita([1]), A. Spataru([1]), D. L. Balabanski([1]), T. Sava([2]), M. Merisanu([1]), T. Roman([1]), C. Scheidenberger([3])([4]), T. Dickel([3])([4]) and W. R. Plass([3])([4])

([1]) *Extreme Light Infrastructure-Nuclear Physics (ELI-NP), "Horia Hulubei" National Institute for Physics and Nuclear Engineering (IFIN-HH) - 30 Reactorului Street, 077125 Magurele, Ilfov, Romania*

([2]) *"Horia Hulubei" National Institute for Physics and Nuclear Engineering (IFIN-HH) 30 Reactorului Street, 077125 Magurele, Ilfov, Romania*

([3]) *II. Physikalisches Institut, Justus-Liebig-Univesitaet Giessen - Giessen, Germany*

([4]) *GSI Helmholtzzentrum fuer Schwerionenforschung GmbH - Darmstadt, Germany*

received 5 February 2019

Summary. — An IGISOL beamline that produces neutron-rich nuclei via photo-fission induced by a high-brilliance gamma beam is being developed at the Extreme Light Infrastructure - Nuclear Physics (ELI-NP) facility. The core device will be a cryogenic stopping cell with an actinide target system in its center. We report on some of the latest simulation results for an optimal design of this gas cell.

1. – Introduction

The ELI-NP project [1, 2] will provide access to two new facilities for nuclear physics with photon beams: two high-power laser systems [3] and a high-brilliance gamma beam system [4].

The IGISOL facility [5] uses the primary gamma beam to generate a secondary Radioactive Isotope Beam (RIB) via photo-fission in UF_4 targets placed at the center of a gas cell filled with He and coupled to a radio-frequency quadrupole (RFQ) for beam formation [6, 7]. The particular technology chosen for the gas cell is that of the High Areal Density with Orthogonal extraction Cryogenic Stopping Cell (HADO-CSC), proposed in Ref. [8], featuring ion extraction orthogonal to the primary beamline. It will be built in collaboration with GSI Darmstadt and Giessen University. The exotic neutron-rich nuclei will be separated, and their mass measured, by a high-resolution Multiple-Reflection Time-of-Flight mass spectrometer. The isomerically pure RIBs [9] will be measured by a β-decay tape station and a collinear laser spectroscopy station.

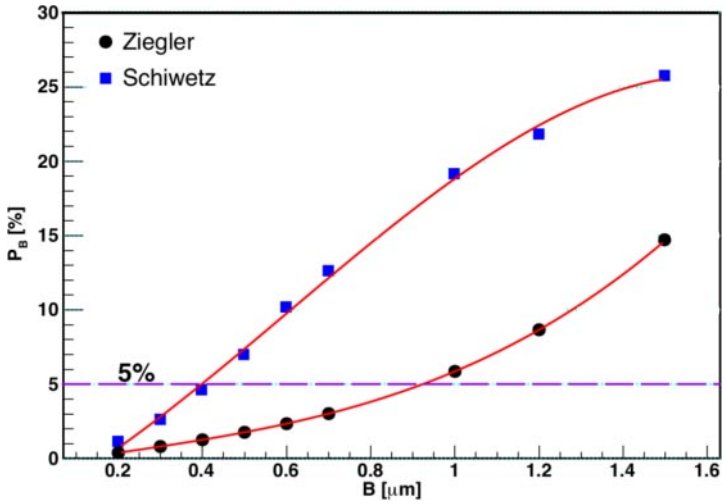

Fig. 1. – Dependence of the percentage P_B of photo-fission fragments stopped in the graphite backing on the layer thickness B. Black circles and blue squares correspond to the Ziegler-Manoyan and the Schiwietz-Grande ionic charge parameterizations, respectively.

This paper continues the work presented in Refs. [6] and [7] with simulations done to optimize various components of the CSC: the target backing, the electric fields for ion extraction, and the supersonic gas jets formed in the nozzles between the two chambers of the HADO-CSC.

2. – New results on CSC simulations

The metallic ^{238}U foils initially proposed for the target system [7] have been replaced with $^{238}UF_4$ foils for chemical and mechanical reasons. Graphite backing on both sides has been included to increase the mechanical strength.

The percentage P_B of photo-fission fragments stopped in the backing layers was estimated for various thicknesses B using the GEANT4 [10] modules described in Ref. [7]. This dependence is shown in Figure 1 for two ionic charge state parameterizations, namely Ziegler-Manoyan [11] and Schiwietz-Grande [12]. Considering a 5% fragment loss acceptable implies using a thickness of 0.4-0.9 μm, depending on the energy loss model used. An optimal value of 0.5 μm for the graphite layer was chosen.

A series of eight RF carpets will be placed on the upper wall of the stopping chamber, as shown in the upper panel of Figure 2, to catch the ions drifted upwards by a DC field acting in the entire volume. Each carpet has concentric electrodes generating an RF field that catches the ions and an additional surface DC field that pushes them towards the nozzle in the center of the carpet, where the gas flow accelerating to supersonic speeds extracts them out of the chamber. A detailed description of the RF carpet of the CSC operating at the Ion Catcher facility at GSI can be found in Ref. [13].

The SIMION program [14] was used to simulate the ion transport on a circular RF carpet similar to that described in Ref. [13]. More specifically, it has 4 electrodes per millimeter, an RF potential of 150 V, and an RF frequency of 6 MHz. An example showing several ions being catched, hovering above the electrodes and pushed towards

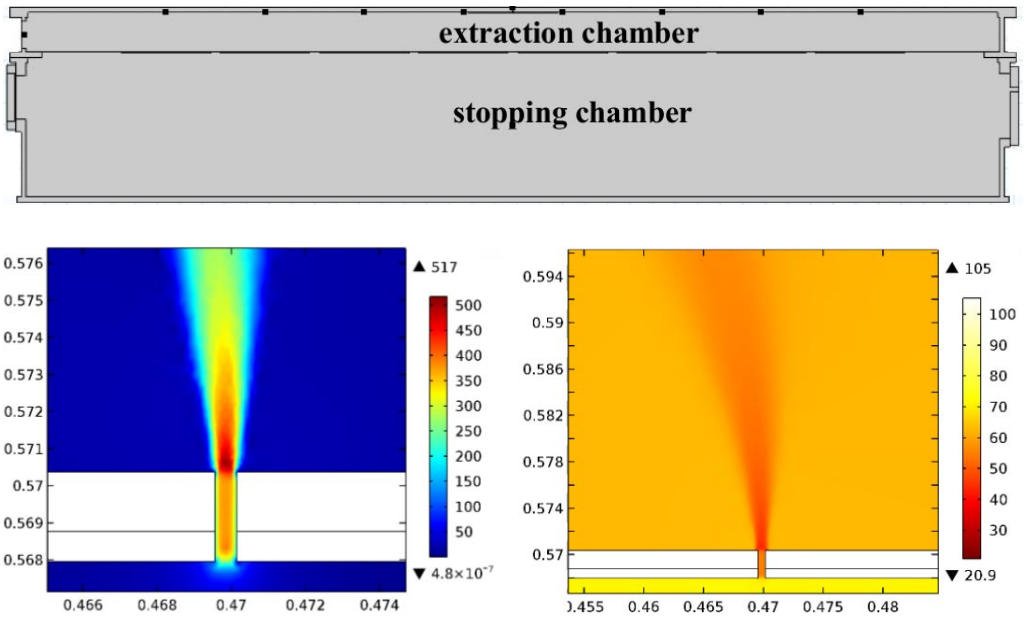

Fig. 2. – Top: CSC geometry used in the COMSOL simulation. Bottom: two-dimensional gas velocity (left) and temperature (right) distributions around one of the eight nozzles between the stopping and extraction chambers.

the nozzle, is presented in Figure 3. Transport efficiencies above 90% and mean times around 10 ms are obtained.

Ions are extracted through the exit nozzles of both chambers by the supersonic gas jets that form due to the large pressure differences and small diameters. The design of the gas system geometry (inlets and outlets) and parameters (pressures and mass flows) has to be done in connection to the properties of these gas jets.

The COMSOL software [15] was used to simulate the gas flow through the CSC. A longitudinal cross-section of the CSC design used is shown in the upper panel of Figure 2. At the inlet, the He gas has a temperature of 75 K and a volumetric flow of 24 l/min. The pressures in the stopping and extraction chambers are 200 mbar and 3 mbar, respectively, while the pressure outside the final extraction nozzle is $5{\cdot}10^{-2}$ mbar. All nozzles have a diameter of 0.6 mm. The resulting two-dimensional gas velocity and

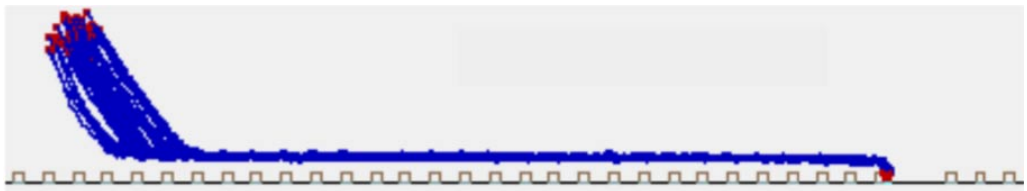

Fig. 3. – Simulation of ion transport above the RF carpet with SIMION. The red dots show the initial and final positions of the ions. The RF carpet described in text catches ions with mass and charge distributions typical for photo-fission fragments and hovers them at about 150 μm.

temperature distributions in one of the nozzles between the two chambers are shown in the bottom left and right panels of Figure 2, respectively. The maximum velocity in the gas jet is 517 m/s and the minimum temperature is 21 K. A decrease in temperature leads to a decrease in the sound velocity v_s:

$$v_s = \sqrt{\frac{\gamma RT}{\mu}} \approx 58.85\sqrt{T} \tag{1}$$

where $\gamma = 5/3$, $R = 8.314 J/(mol \cdot K)$, and $\mu = 4 \cdot 10^{-3} kg/mol$ are the adiabatic constant, the gas constant, and the atomic mass of helium. Consequently, the velocity increase coupled to the temperature decrease lead to supersonic jets, the Mach number reaching $M = v/v_s = 1.92$ in this case.

3. – Conclusion

The main directions that are currently pursued in finalizing the design of the HADO-CSC components have been presented. While some of them are finished or in very advance stages, like the target system and the gas system, others need more study, like the RF carpets. Detailed reports of these developments will be published in future papers.

* * *

This work was supported by Extreme Light Infrastructure Nuclear Physics (ELI-NP) Phase II, a project co-financed by the Romanian Government and the European Union through the European Regional Development Fund - the Competitiveness Operational Programme (1/07.07.2016, COP, ID 1334). The ELI-RO project is supported by the Romanian Government through the Grant Programme ELI-RO-07.

REFERENCES

[1] Zamfir N.V., *Nuclear Physics News* **25** (2015) 34.
[2] Balabanski D.L. *et al.*, *Eur. Phys. Lett.* **117** (2017) 28001.
[3] Ursescu D. *et al.*, *Proc. of SPIE* **8780** (2013) 87801H-1.
[4] Weller H.R. *et al.*, *Rom. Rep. Phys.* **68** (2016) S447.
[5] Balabanski D.L. *et al.*, *Rom. Rep. Phys.* **68** (2016) S621.
[6] Constantin P. *et al.*, *Nucl. Inst. Meth. B* **372** (2016) 78.
[7] Constantin P. *et al.*, *Nucl. Inst. Meth. B* **397** (2017) 1.
[8] Dickel T. *et al.*, *Nucl. Inst. Meth. B* **376** (2016) 216.
[9] Dickel T. *et al.*, *Phys. Lett. B* **744** (2015) 137.
[10] Agostinelli S. *et al.*, *Nucl. Instr. Meth. A* **506** (2003) 250.
[11] Ziegler J.F. and Manoyan J.M., *Nucl. Instrum. Methods B* **35** (1988) 215.
[12] Schiwietz G. and Grande P.L., *Nucl. Instrum. Methods B* **175-177** (2001) 125.
[13] Ranjan M. *et al.*, *Nucl. Inst. Methods A* **770** (2015) 87.
[14] Manura D. and Dahl D., SIMION 8.0 User Manual, Sci. Instrum. Serv. Inc., 2008.
[15] www.comsol.com